

# Mechanical and Thermal Properties of Polymethylmethacrylate Bone Cement Composites Incorporated with Hydroxyapatite and Glass-Ceramic Fillers

A. S. Hamizah,<sup>1</sup> M. Mariatti,<sup>1</sup> R. Othman,<sup>1</sup> M. Kawashita,<sup>2</sup> A. R. Noor Hayati<sup>3</sup>

<sup>1</sup>*School of Materials & Mineral Resources Engineering, Universiti Sains Malaysia, Engineering Campus, 14300 Nibong Tebal, Penang, Malaysia*

<sup>2</sup>*Graduate School of Biomedical Engineering, Tohoku University, 6-6-11-1306-1 Aramaki-Aoba, Aoba, Sendai 980-8579, Japan*

<sup>3</sup>*School of Dental Sciences, Universiti Sains Malaysia, Healthy Campus, 16150 Kubang Kerian, Kelantan, Malaysia*

Received 9 December 2010; accepted 17 July 2011

DOI 10.1002/app.35295

Published online 7 February 2012 in Wiley Online Library (wileyonlinelibrary.com).

**ABSTRACT:** A new bioactive glass-ceramic based on the  $\text{Na}_2\text{O}-\text{CaO}-\text{SiO}_2-\text{P}_2\text{O}_5$  glass system was used as bioactive filler in commercial polymethylmethacrylate (PMMA) bone cement; (PALACOS<sup>®</sup> LV). The results of this newly fabricated glass-ceramic were compared with those of hydroxyapatite (HA) filler. PMMA bone cement containing 0, 4, 8, 12, or 16 wt % glass-ceramic and HA were prepared. The effects of bioactive fillers and different filler loadings on mechanical and thermal properties were evaluated. Results show that flexural strength decreased, while flexural modulus increased as filler loading was amplified. Fracture toughness was also observed. Results of thermogravimetric analysis indicate that the thermal stability of the cement composites increased with increasing glass-ceramic and HA contents. Dynamic mechanical analysis shows that the addition of glass-ceramic fillers resulted in an increase in storage modulus and  $T_g$ . Apatite morphology was observed on the surface of the glass-ceramic, GCBC4, and GCBC8 after a bioactivity test. © 2012 Wiley Periodicals, Inc. *J Appl Polym Sci* 125: E661–E669, 2012

**Key words:** composites; biomaterials; filler; thermal properties; thermogravimetric analysis

## INTRODUCTION

Polymethylmethacrylate (PMMA) bone cements have been in the market for almost 50 years since their introduction by Sir John Charnley.<sup>1,2</sup> They have been widely used in dentistry and orthopedic surgery for dental cavity filling and fixation of total joint prosthesis of the bone.<sup>2,3</sup> However, conventional bone cements exhibit drawbacks such as poor mechanical properties, inability to bond with bones, high exothermic polymerization temperatures, release of residual monomer, and high shrinkage.<sup>4,5</sup> Therefore, a large number of studies are being carried out on the development of bone cement formulation to improve the mechanical, thermal, handling, and biocompatibility properties of bone cements.

Current research on bone cements has focused on the incorporation of bioactive fillers, such as hydroxyapatite (HA),  $\beta$ -tricalcium phosphate,<sup>6,7</sup> titania,<sup>8</sup> bioactive glasses,<sup>9</sup> and bioactive glass-ceramics,<sup>10,11</sup> in PMMA bone cement. As a result, bioactive bone cement composites based on modified PMMA composites have been developed. These bioactive composites are proven advantageous in producing an intermediate region between bones and prostheses. They possess excellent osteoconductivity and better mechanical properties than does conventional PMMA bone cement.<sup>6–11</sup> Bioactive materials can bond to living bones in the body through the formation of an apatite layer on their surfaces. When these materials are implanted into the bone, the apatite formed on the surface of the newly-formed bone tissue fills the gap between the surrounding bone and the apatite layer.<sup>12</sup> In previous work, a nucleation and growth mechanism of an apatite-like layer on bioactive materials containing  $\text{CaO}-\text{SiO}_2$  has been proposed and experimentally confirmed in most bioactive glasses and glass-ceramics.<sup>13,14</sup>

In this study, the effect of incorporating bioactive glass-ceramic particles ( $\text{Na}_2\text{O}-\text{CaO}-\text{SiO}_2-\text{P}_2\text{O}_5$ )

Correspondence to: M. Mariatti (mariatti@eng.usm.my).

Contract grant sponsor: Ministry of Science, Technology, and Innovation, Malaysia (MOSTI); contract grant number: 12-01-05-SF0316.

Contract grant sponsors: Universiti Sains Malaysia; National Science Fellowship (NSF) Scheme.

into commercial PMMA bone cement was investigated. The bioactive glass-ceramic was produced based on a new formulation. Glass-ceramic materials are fine grained polycrystalline solids containing residual glass phase, produced by melting glass and forming it into products that are subjected to controlled crystallization. To date, no other study has been conducted on the properties of this bioactive glass-ceramic as filler in PMMA bone cements. The mechanical and thermal properties obtained were compared with those of HA particle-filled bone cement composites. HA is a natural mineral form of apatites with the formula  $\text{Ca}_{10}(\text{PO}_4)_6(\text{OH})_2$  and the structure of HA is hexagonal.

## MATERIAL AND EXPERIMENTAL

### Preparation of bioactive fillers

The glass composition of  $55\text{SiO}_2$ ,  $10\text{Na}_2\text{O}$ , and  $35\text{CaO}$  (wt %) was synthesized. The chosen composition was based on glass formation in the ternary phase equilibrium diagram of  $\text{SiO}_2\text{--Na}_2\text{O--CaO}$ .<sup>15</sup> A 3 wt % of  $\text{P}_2\text{O}_5$  was added in the glass composition to act as nucleating agent. The glass powder was then heat-treated at a nucleation temperature of  $600^\circ\text{C}$  for 1 h, and subsequently heated to  $950^\circ\text{C}$  for crystallization at a heating rate of  $5^\circ\text{C}/\text{min}$  followed by natural cooling in a furnace. The glass-ceramic was then pulverized by zirconia ball milling, resulting in an irregularly shaped glass-ceramic powder. The density of the glass-ceramic powder was  $2.528 \pm 0.009 \text{ g}/\text{cm}^3$ , and the average particle size was  $\sim 12.64 \pm 0.80 \mu\text{m}$ . The density and particle size of glass-ceramic fillers were measured using a Presica XT 220A and Sympatec-HELOS system laser diffraction analyzer, respectively.

Commercially available HA powder was used as referential filler. Pure crystalline HA powder was supplied by Sigma Aldrich. The shape of the HA powder was spherical. The density and average particle size were  $3.140 \text{ g}/\text{cm}^3$  (given by supplier) and  $5.46 \pm 0.40 \mu\text{m}$ , respectively. However, the actual particle size of the HA provided by the supplier was 200 nm, suggesting that the HA particles consisted of agglomerates.

### Preparation of bone cement composites

Commercial bone cement (PALACOS<sup>®</sup> LV supplied by Heraeus Kulzer GmbH) was used as matrix. As reported by the supplier, each dose of surgical bone cement contained 40 g of PMMA powder and 20 g of liquid monomer, with a powder-to-liquid ratio of 2 : 1. The compositions of PALACOS<sup>®</sup> LV bone cement are shown in Table I. Benzoyl peroxide (BPO) acts as an initiator for liquid MMA in the

TABLE I  
Composition of PALACOS<sup>®</sup> LV Bone Cement

Component	Composition	Weight (g)
Powder	PMMA	33.6
	Zirconium dioxide	6.0
	Benzoyl peroxide	0.4
Liquid	Methyl methacrylate (MMA)	18.4
	<i>N,N</i> -Dimethyl- <i>p</i> -toluidine	0.4
	Colourant E141 and hydroquinone	1.2

polymerization reaction to initiate the curing of the cement. Zirconium oxide ( $\text{ZrO}_2$ ) is used as a radiopacifier, and it is commonly been added in the powder component to confer radiopacity and thus aid in the radiographic assessment of the cement. While, in the liquid component, *N,N*-dimethyl-*p*-toluidine (DMPT) is functions as an activator or accelerator in the polymerization reaction and hydroquinone (HQ) is added to act as inhibitor to avoid a premature polymerization. Different weight fractions of as-fabricated glass-ceramics and HA were prepared by adding these fillers to the liquid monomer prior to mixing both components. All bone cements were prepared by mixing the solid and liquid components using a Stryker Mixevac III bowl under vacuum for 2–3 min until consistency was similar to that of dough. Vacuum condition is important to prevent air entrapment in cement and to reduce bone cement porosity. The specimen was then cast in a stainless steel mold and allowed to cure for 1 h at room temperature. Different compositions were prepared by adding various amounts of glass-ceramics and HA, as shown in Table II.

## Characterization

### Flexural test

A flexural test was performed to examine the mechanical properties of the prepared bone cement samples. The cured cement was cut into bars of rectangular cross-sections with dimensions of  $90 \times 12.7 \times 3 \text{ mm}^3$ , as recommended by ASTM D790-03.<sup>16</sup> The test was conducted at a cross-head speed of 5 mm/min at room temperature, and the support length was set to 50 mm. For each sample, at least five specimens were tested and average values were obtained. Young's modulus and flexural strength were calculated from the load versus the displacement curve. Results were computed using the following standard formulas:

$$\text{Young's modulus, } E = L^3M/4bd^3 \quad (1)$$

$$\text{Flexural strength, } S_{\text{max}} = 3PL/2bd^3 \quad (2)$$

where  $L$  is the distance between the supports ( $m$ ),  $P$  is a load at a given point on the load deflection

**TABLE II**  
**Mixing Composition of Particulate Filler-Filled PMMA Bone Cement**

Sample	Filler loading (wt %)	Powder parts		Liquid parts (mL)	Liquid to powder (L/P) ratio
		PMMA powder (g)	Filler (g)		
Control	0	40	–	20	0.5
HABC4	4	40	1.6	20	0.48
HABC8	8	40	3.2	20	0.46
HABC12	12	40	4.8	20	0.45
HABC16	16	40	6.4	20	0.43
GCBC4	4	40	1.6	20	0.48
GCBC8	8	40	3.2	20	0.46
GCBC12	12	40	4.8	20	0.45
GCBC16	16	40	6.4	20	0.43

curve,  $M$  is the gradient of the initial straight-line portion of the load deflection curve ( $N/m$ ),  $b$  represents the width of the specimen ( $m$ ), and  $d$  denotes the thickness of the specimen ( $m$ ). The test was performed using an Instron Universal Testing Machine (model 3366, Instron).

#### Fracture toughness

The single-edge-notched-beam test was carried out using the universal testing machine to measure the fracture toughness of the bone cement samples. The dimensions of the test specimen were  $74 \times 12.5 \times 3 \text{ mm}^3$ . Five specimens were prepared for each type of bone cement sample. For each specimen, a notch of 5.6 mm in depth was created on one side using a band saw. A support span length of 51 mm was used with a cross-head speed of 1.00 mm/min. The value of plain-strain fracture toughness ( $K_{IC}$ ) of each specimen was calculated via eq. (3).

$$K_{IC} = \frac{3PSa^{1/2}y}{2tw^2} \quad (3)$$

where  $K_{IC}$  = plain-strain fracture toughness of the test specimen, ( $\text{MPa m}^{1/2}$ ),  $P$  is the load at peak,  $S$  represents the support span length,  $a$  is the notch length,  $t$  is the specimen thickness,  $w$  denotes the specimen width, and  $y$  is the geometrical correction factor.

#### Scanning electron microscopy

The fractured surfaces of the composite cements from the flexural-tested samples were examined by SEM using a Zeiss Supra<sup>TM</sup> 35VP instrument. All specimens were sputtered with a thin gold layer for electron reflection prior to SEM examination. SEM (VE-8800, Keyence, Tokyo, Japan) was also used to

characterize the surface morphologies of the glass-ceramic and bone cement composite samples (GCBC4 and GCBC8) after soaking in simulated body fluid (SBF) solution for 7 days. The characterization was performed at Tohoku University.

#### Thin-film X-ray diffraction

TF-XRD (RINT-2200VL; Rigaku, Tokyo, Japan) was carried out to investigate apatite formation on the cement samples with 4 and 8 wt % of glass-ceramic filler loadings (GCBC4 and GCBC8). The TF-XRD measurements were performed using Ni-filtered  $\text{CuK}_\alpha$  radiation as the X-ray source at a rate of  $2\theta = 2^\circ/\text{min}$  and sampling angle of  $0.02^\circ$  against the incident beam on the sample surface. Data were collected from  $10^\circ$  to  $60^\circ$ , and the characterization was conducted at Tohoku University.

#### Thermogravimetric analysis

TGA of the PMMA bone cement and PMMA bone cement composites was carried out by using a thermogravimetric analyzer (Perkin Elmer-TGA 6) with temperature programmed at  $10^\circ\text{C}/\text{min}$  heating rate, from 30 to  $600^\circ\text{C}$  in a nitrogen atmosphere. About 5–10 mg of the samples has been used for TGA testing.

#### Dynamic mechanical analysis

The Dynamic Mechanical Analysis (DMA) properties of cured samples were determined in the temperature range of  $30\text{--}120^\circ\text{C}$ . The measurement was carried out using a Mettler Toledo (model DMA 861e) dynamical mechanical analyzer operated under a three-point bending configuration. The beam measuring  $10 \times 2 \times 50 \text{ mm}^3$  was used. The oscillating force was set to 0.1 Nm with a displacement of 20  $\mu\text{m}$ . The frequency and heating rate were set to 1 Hz and  $10^\circ\text{C}/\text{min}$ , respectively.

## RESULTS AND DISCUSSION

### Flexural properties of the PMMA bone cement composites

The typical stress–strain behavior from the flexural tests of the PMMA bone cement incorporated with glass-ceramic and HA, is shown in Figure 1. On the basis of the stress-strain curve, no plastic deformation was observed beyond the elastic region occurring for samples incorporated with a high filler loading (16 wt %). The samples (GCBC16 and HABC16) failed immediately after the flexural stress reached a maximum value. All of the filled bone cement samples showed the same mode of failure, that is, brittle failure. However, the sample with 16 wt % filler



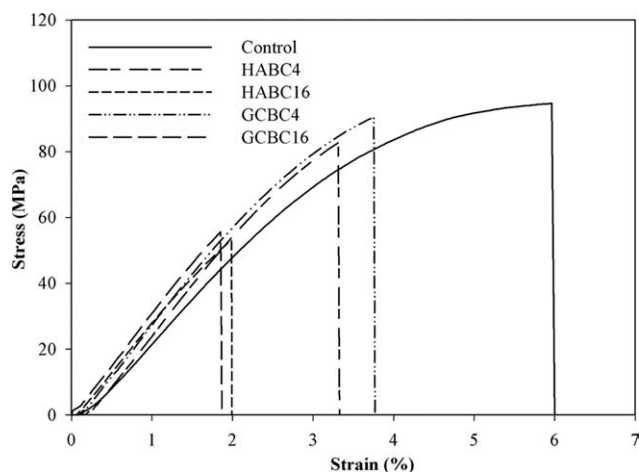


**Figure 1** Stress versus strain of selected PMMA bone cement composites and PMMA cement (as control).

loading broke at a higher strain compared with that with 4 wt %.

The results of the average flexural modulus test are shown in Figure 2. The Young's moduli of the GCBC and HABC composites increased monotonically as the proportion of fillers increased. By adding 16 wt % of filler, the flexural modulus increased by ~ 22% and 19.7% in GCBC and HABC, respectively, compared with unfilled cement. The GCBC composites show higher flexural moduli at the same filler loading as that of the HABC samples. According to Endogan et al.<sup>3</sup> the elastic modulus of the composites increased with the addition of filler loading because the polymeric matrix contains an inorganic material of stiff structure. Thus, the presence of glass-ceramic and HA enhances the values of the elastic modulus compared with cement having none of these particles. Theoretically, the modulus of elasticity of bone cement should not be lower than the

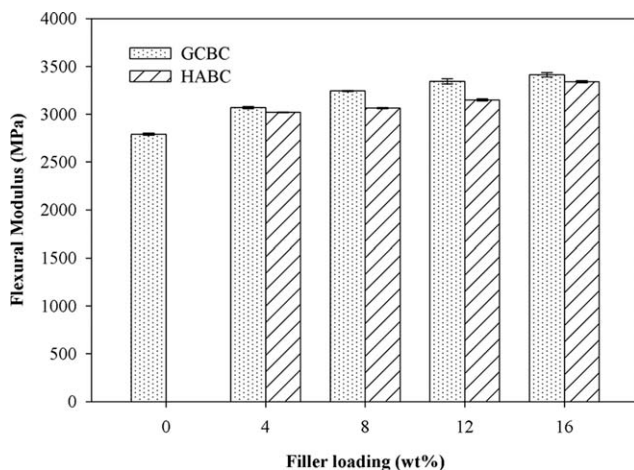


**Figure 2** Effect of filler loading on flexural modulus of GCBC and HABC samples at 4 to 16 wt % of fillers (0wt % is a control sample).

modulus of the metallic prosthesis and the bone to effectively act as a mechanical buffer. This result is in agreement with the increase in Young's modulus reported in literature.<sup>4,9,17</sup>

Figure 3 shows the bar chart of the flexural strength of GCBC and HABC. Flexural strength decreased with an increase in filler loading. For example, the addition of 4 wt % glass-ceramic filler resulted in a 9.6% reduction in flexural strength, whereas a 13.3% reduction was generated by the addition of 16 wt % glass-ceramic. The decrease may be attributed to the high viscosity of the initial dough and mixing difficulties, which resulted in particle agglomerations or filler clusters in the cement samples.<sup>18,19</sup> This subsequently introduced a weak point in the cement, thereby decreasing its flexural strength. At the same filler loading, the HABC composites showed a lower trend of flexural strength compared with the GCBC composites. This is due to the small size of HA particles, which exhibited a higher surface area, and subsequently resulted in more agglomeration compared with glass-ceramic particles. Figure 4 shows the agglomeration of filler particles (glass-ceramic and HA) in the bone cement composite.<sup>4,18,20</sup>

### Fracture toughness

The fracture toughness ( $K_{IC}$ ) of the bone cements incorporated with glass-ceramic and HA fillers decreased as filler loading increased, as shown in Figure 5. In this case, the fracture toughness of GCBC is lower than that of HABC, which may be due to the shape of the filler particles. As indicated in Section "Preparation of bioactive fillers", the GCBC particles were prepared by ball milling process, which resulted in an irregular shape with sharp edges. These edges act as stress concentration components and increase the possibility of cement

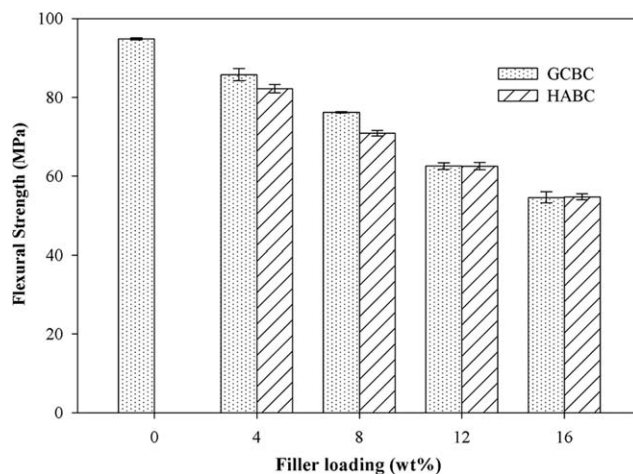


**Figure 3** Effect of filler loading on flexural strength of GCBC and HABC samples at 4 to 16 wt % of fillers (0wt % is a control sample).

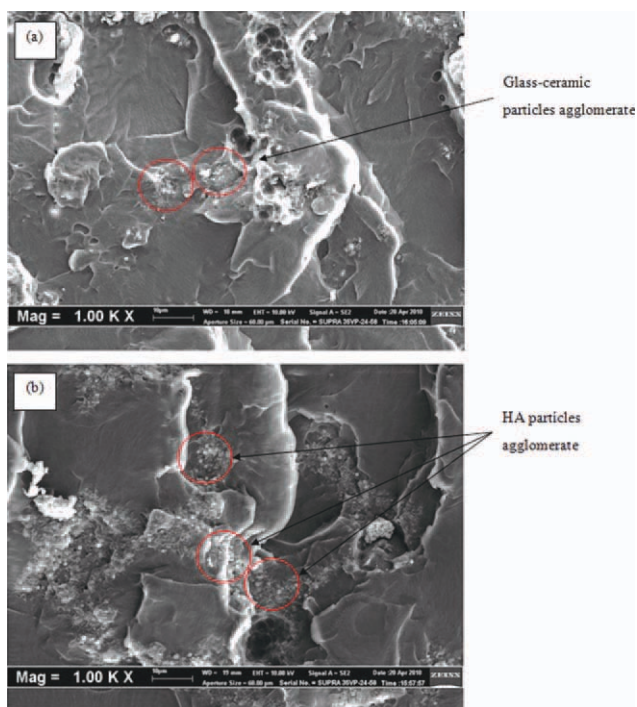


**Figure 4** SEM images of the (a) GCBC16 (b) HABC16 at magnification of 1K X. [Color figure can be viewed in the online issue, which is available at wileyonlinelibrary.com.]

failure, hence reducing fracture toughness.<sup>18</sup> The fracture toughness of the GCBC samples with filler concentrations of more than 8 wt % is approximately similar; thus, the effect of filler loading is negligible.

**TGA**

The thermal stability of the PMMA bone cement composites has been studied by means of thermogravimetric analysis. The weight loss curve and the derivative weight (DTG) curves for bone cement

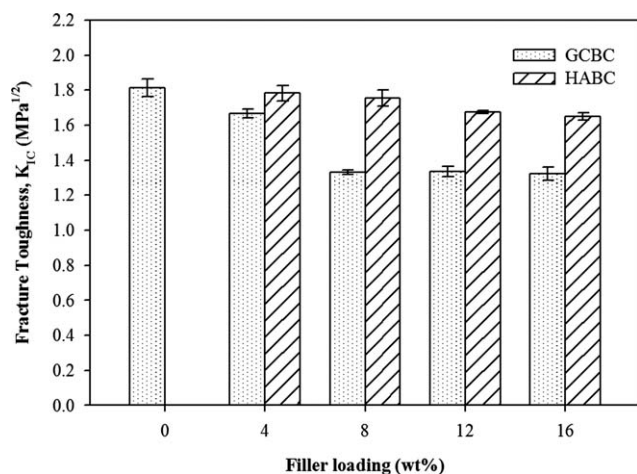


**Figure 5** Effect of filler loading on fracture toughness of GCBC and HABC samples at 4 to 16 wt % of fillers (0wt % is a control sample).

composites with 4 and 16 wt % of filler, compared to control, are reported in Figure 6 and the data is shown in Table III. On the basis of weight loss curve in Figure 6(a), the TGA curves leveled off at temperatures higher than 430°C, implying little weight loss beyond this temperature. For the control sample, the residue content at 600°C was 10.12%, caused by the existence of ZrO<sub>2</sub> that acted as a radiopacifier in the powder component, which did not burn under the tested temperature range.

From Figure 6(a), it can be seen that the weight loss of all samples occurred in a one-step degradation process from 200°C to less than 430°C. This result confirmed by the presence of only one peak in DTG curve as shown in Figure 6(b). Note that the peak point of the DTG curve is referring to the inflection temperature and higher value of inflection temperature indicates higher thermal stability. From the DTG curves in Figure 6(b) and the data in Table III, it is observed that the inflection temperature of PMMA bone cement composites is higher than

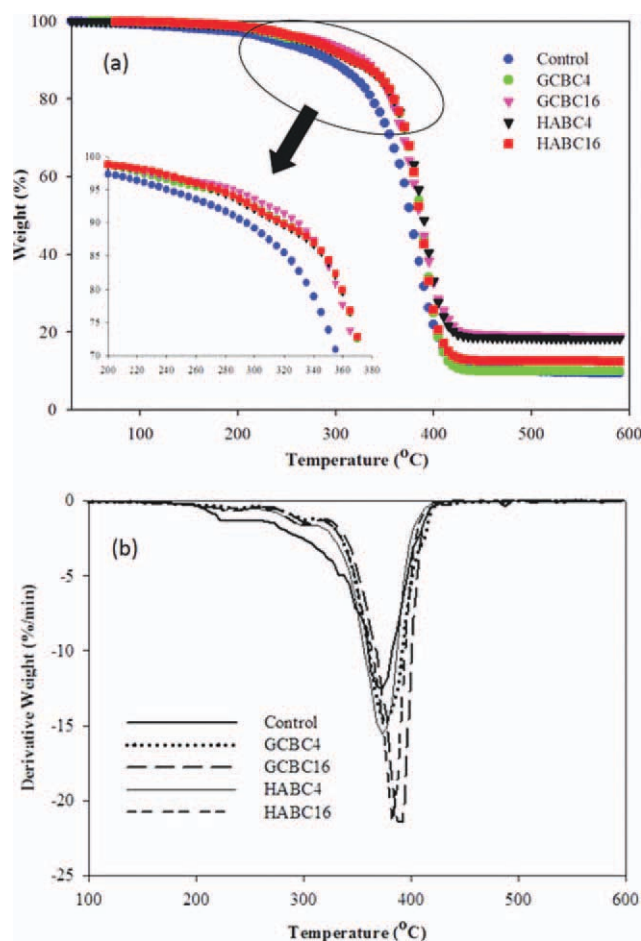


**Figure 6** TGA analysis of control, GCBC, and HABC composites with 4 and 16 wt % of filler loadings; (a) weight vs temperature, (b) derivative weight vs temperature. [Color figure can be viewed in the online issue, which is available at wileyonlinelibrary.com.]

**TABLE III**  
**TGA Analysis of PMMA Bone Cement Composite (Control sample refers to the 0wt %)**

Sample	Inflection temperature (°C)	Mass loss at inflection temperature (%)	Mass loss content at 300°C (%)	Mass loss content at 400°C (%)	Residue content at 600°C (%)
Control	372.5	12.59	10.89	78.12	10.12
GCBC4	377.5	14.83	7.52	74.98	13.22
GCBC16	392.5	21.44	6.43	67.21	20.41
HABC4	375.5	15.52	7.97	74.24	12.36
HABC16	382.5	21.32	7.71	66.16	21.39

control sample. The inflection temperature is shifted from 372.5°C for control to 392.5°C and 382.5°C for GCBC and HABC with 16 wt % of filler loading, respectively. It is evident that the thermal stability enhancement can be attributed by the presence of glass-ceramic and HA filler in PMMA bone cement.

The thermal stability of GCBC composites tended to increase significantly with increases in glass-ceramic content from 4 to 16 wt % if compared to the HABC composite. The filler seems to successfully act in these composites by restricting the movement of the chain segment in the PMMA matrix during the thermal degradation of the composites. This result agrees with those of Yang et al.<sup>21</sup> which showed that the thermal stability of bone cement increased with increasing tri-calcium phosphate (TCP) content. The trend of increasing inflection point of the HABC sample added with HA in the bone cement composite was observed. However, the value is not significantly increased.

## DMA

Figure 7 represents the storage modulus of the GCBC and HABC composites, compared with com-

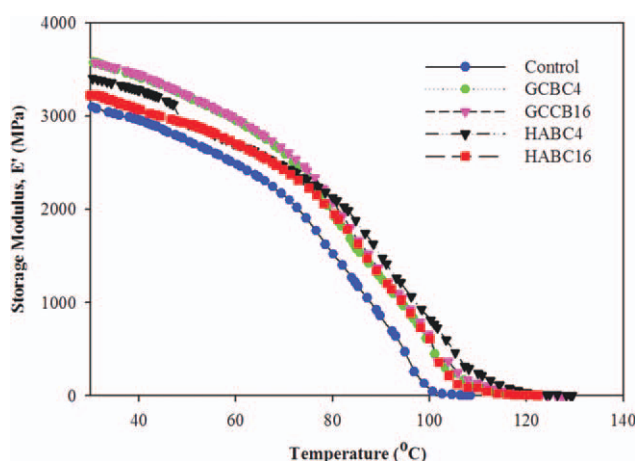


**Figure 7** Storage modulus as a function of temperature for control, GCBC, and HABC composites with 4 and 16 wt % of filler loadings (control sample refers to the 0wt %). [Color figure can be viewed in the online issue, which is available at [wileyonlinelibrary.com](http://wileyonlinelibrary.com).]

mercial PMMA bone cement. The control sample exhibited a much lower storage modulus than did the cement samples at 30°C. Storage modulus, however, increased upon the addition of glass-ceramic filler from 3098 MPa for commercial PMMA bone cement to 3573 and 3593 MPa for GCBC4 and GCBC16, respectively. The same observation was noted for the HABC composites. The addition of glass-ceramic and HA as rigid inorganic components improved the stiffness of the PMMA matrix in the commercial bone cement. In other words, the presence of ceramic fillers enables the matrix to sustain a high modulus at high temperatures. The trend is consistent with the flexural modulus obtained from the static flexural tests as discussed in Section “Flexural properties of the PMMA bone cement composites”.

Tan delta is an indication of molecular motions existing in materials. A comparison of tan delta as a function of temperature for commercial bone cement and its composites (GCBC and HABC) are shown in Figure 8. Under the analyzed temperature range, the tan delta curves of all the samples are characterized by only one relaxation located at the range 90–120°C. This relaxation is known as beta-transition.

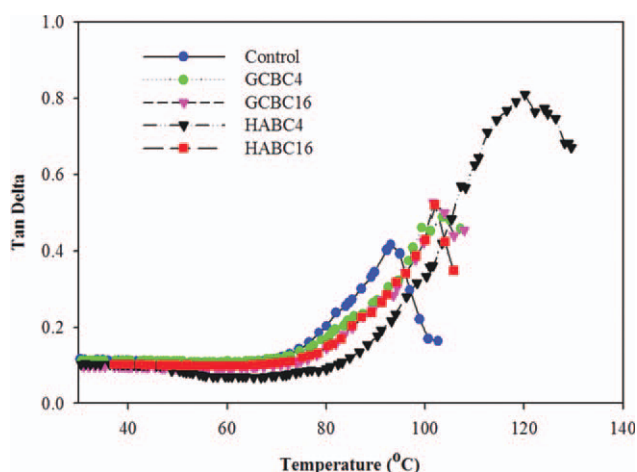


**Figure 8** Tan delta as a function of temperature for control, GCBC, and HABC composites with 4 and 16 wt % of filler loadings (control sample refers to the 0wt %). [Color figure can be viewed in the online issue, which is available at [wileyonlinelibrary.com](http://wileyonlinelibrary.com).]



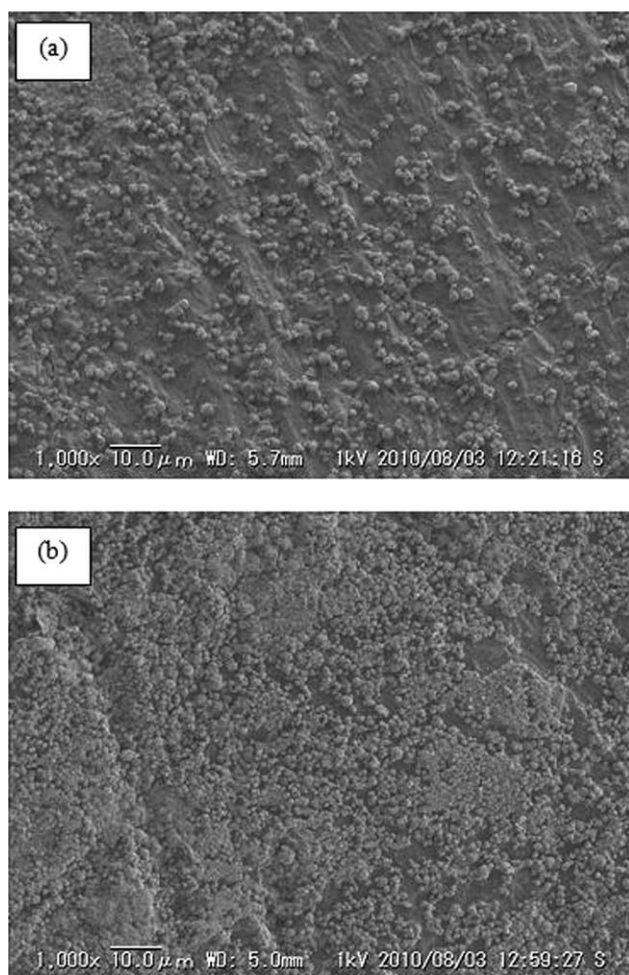


**Figure 9** SEM images of the (a) GCBC4 (b) GCBC8 after soaking in SBF for 7 days at magnification of 1K X.

According to Cheng et al.<sup>22</sup> the position of the primary beta-transition peak can be related to the interaction between the amorphous PMMA chains and inorganic filler at the molecular level. Figure 8 also shows that the tan delta value of the GCBC composite increased with the incorporation of glass-ceramic filler. Generally, the increase in peak amplitude of the tan delta indicates a decrease in chain mobility, and the peak amplitude can be related to the amount of amorphous PMMA chains involved in the transition.<sup>22</sup> A contrasting result was observed for the HABC composites, in which the tan delta value decreased upon the incorporation of 16 wt % HA. The decrease in tan delta is due to the restricted mobility of the polymer chains by the dispersed rigid of agglomerate nanofillers in the system.<sup>23</sup>

The glass transition ( $T_g$ ) of a sample can be deduced from the position peak of the tan delta curve (Fig. 8). The value of  $T_g$  of the PMMA bone cement composite was much higher than that of the control sample, which yielded a  $T_g$  of 93.1°C. This

indicates that the peak moves to a slightly higher temperature with increasing glass-ceramic and HA contents, showing that the  $T_g$  of the composite increases with the addition of fillers. In other words, glass-ceramic and HA fillers hinder the segmental motion of the PMMA chains. However, when filler loading increased from 4 wt % to the maximum load (16 wt %), the  $T_g$  of GCBC composites slightly decreased by 1.8°C. While in HABC composites system, the  $T_g$  decreased by 18.1°C with addition of filler from 4 to 16 wt %. At high filler concentration, the number of free volumes or voids increases due to the high viscosity of the dough. As indicated in Section "Flexural properties of the PMMA bone cement composites", more agglomeration or filler-to-filler interaction were observed in HABC compared to GCBC. This results in high voids in HABC which subsequently reduced the  $T_g$  of the PMMA cement.

#### Bioactivity test

On the basis of the mechanical and thermal properties of the PMMA bone cement composite, 4 and 8 wt % of glass-ceramics samples (GCBC4 and GCBC8, respectively) were chosen for the bioactivity test by soaking in SBF solution. SEM and TF-XRD techniques were used to analyze apatite layer development on the glass-ceramic and cement composite. Figure 9 shows the SEM micrographs of GCBC4 and GCBC8. Apatite globules were formed on the surface of the cement samples. For the GCBC sample with a higher filler loading of glass-ceramics (GCBC8), more apatite globules were observed on the surface [Fig. 9(b)].

Figure 10 shows the TF-XRD patterns of glass-ceramic heat-treated at 950°C, before and after 7 days of soaking in SBF. TF-XRD patterns for cement samples (GCBC4 and GCBC8) after soaking are also

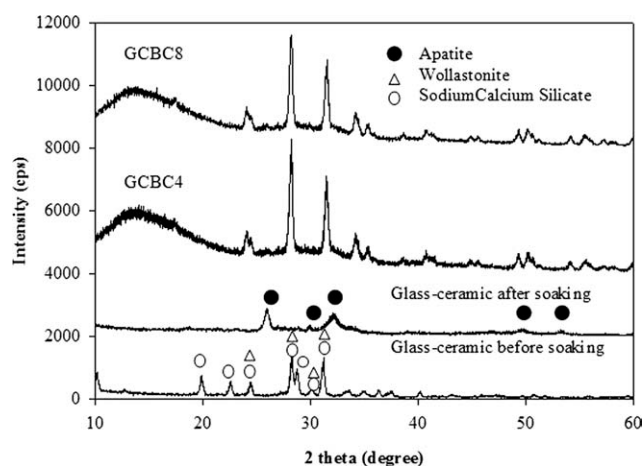


**Figure 10** TF-XRD patterns of bioactive glass-ceramic, GCBC4, and GCBC8 cement sample after soaking in SBF for 7 days.

**TABLE IV**  
**Summary Results of PMMA Bone Cement Composites Studied in Previous Works**

References	Types of filler	Optimum filler loading (wt %)	Flexural strength (MPa)	Flexural modulus (GPa)	Fracture toughness (MPa m <sup>1/2</sup> )
Shinzato et al. [9]	Glass bead	60	135 ± 4	5.8 ± 0.1	–
Goto et al. [8]	Micron-sized titania particles	56	69.3 ± 6.6	4.07 ± 0.83	–
Jasso-Gastinel et al. [4]	Cuttlebone particles- <i>Sepia officinalis</i>	10	56	3.2	1.29 ± 0.04
		30	54	3.2	1.11 ± 0.03
Khaled et al. [24]	Titania nanotubes	1.0	90.73	3.81	1.42 ± 0.09
Present study	Bioactive glass ceramic	4	85.78 ± 1.53	3.06 ± 11	1.667 ± 0.027
		8	76.21 ± 0.21	3.24 ± 6	1.330 ± 0.013
Present study	HA	4	82.23 ± 1.08	3.02 ± 4	1.782 ± 0.043
		8	70.92 ± 0.71	3.07 ± 6	1.757 ± 0.046

presented in Figure 10. For glass-ceramic after soaking, the low peak intensities of apatite was clearly formed on the surface at  $2\theta = 26^\circ, 30^\circ, 32^\circ, 50^\circ,$  and  $54^\circ$ . A broad *halo* peak was observed in the range of  $2\theta = 10^\circ$  to  $23^\circ$  on the both cement samples (GCBC4 and GCBC8). This peak is belongs to polymer matrix (PMMA) as indicated in the TF-XRD as amorphous phases. For GCBC4 and GCBC8, sharp peaks of the main crystalline phases corresponded to wollastonite ( $\text{CaSiO}_3$ ) and sodium calcium silicate ( $\text{Na}_2\text{Ca}_3\text{Si}_6\text{O}_{16}$ ) presented at  $2\theta = 24^\circ, 28^\circ,$  and  $31^\circ$ . These phases are found to be similar with the phases exist in glass-ceramic before soaking in SBF solution.

Conversely, no sign of apatite was detected in the GCBC4 and GCBC8 samples. The amount of glass-ceramics in the cement is suspected as insufficient. Furthermore, high viscosity of the mixture incorporated with fillers occurred during the mixing process, causing uneven distribution of glass-ceramics in the cement sample. The combination of uneven filler distribution and the small size of TF-XRD sample testing may result in unsuccessful detection of the apatite peak in cement samples by TF-XRD.

Table IV shows a comparison of the different filler-filled bone cement composites based on previous studies. The GCBC and HABC (4 and 8 wt %) composites were chosen as comparison standards because of their optimal mechanical and thermal properties. Generally, the results obtained from the present study are comparable with those of previous work even though a small amount of filler was applied in this research. In short, PMMA bone cement containing  $\text{Na}_2\text{O}-\text{CaO}-\text{SiO}_2-\text{P}_2\text{O}_5$  glass-ceramic particles is a promising type of bone cement for prosthesis fixation, but further research on using a higher amount of bioactive glass-ceramic should be performed.

## CONCLUSIONS

In this article, a new composition of glass-ceramic was used as bioactive filler in PALACOS<sup>®</sup> LV. The GCBC sample showed a higher flexural strength and

flexural modulus than did HABC. Increasing filler loading resulted in an increase in flexural modulus, but a decrease in flexural strength. The thermal stability of the GCBC composite also increased with an increase in glass-ceramic content. The storage modulus in DMA analysis showed an increment, and  $T_g$  increased with the addition of glass-ceramic fillers. Overall, this research showed that bone cement containing 4 and 8 wt % glass-ceramic filler loading exhibited optimum mechanical and thermal properties when compared with HA fillers.

## References

- Lewis, G. J *Biomed Mater Res Part B: Appl Biomater* 1997, 38, 155.
- Kuehn, K. D.; Ege, W.; Gopp, U. *Orthop Clin North Am* 2005, 36, 17.
- Endogan, T.; Serbetci, K.; Hasirci, N. *J Appl Polym Sci* 2009, 113, 4077.
- Jasso-Gastinel, C. F.; Reyes-Gonzalez, I.; Enriquez, S. G.; Flores, J.; Mijares, E. M. *Macromol Symp* 2009, 283/284, 159.
- Basgorenay, B.; Ulubayram, K.; Serbetci, K.; Onurhan, E.; Hasirci, N. *J Appl Polym Sci* 2006, 99, 3631.
- Wang, C. X.; Tong, J. *Biomed Mater Eng* 2008, 18, 367.
- Canul-Chuil, A.; Vargas-Coronado, R.; Cauich-Rodríguez, J. V.; Martínez-Richa, A.; Fernández, E.; Nazhat, S. N. *J Biomed Mater Res* 2003, 64, 27.
- Goto, K.; Hashimoto, M.; Takadama, H.; Tamura, J.; Fujibayashi, S.; Kawanabe, K.; Kokubo, T.; Nakamura, T. *J Mater Sci: Mater Med* 2008, 19, 1009.
- Shinzato, S.; Nakamura, T.; Kokubo, T.; Kitamura, Y. *J Biomed Mater Res* 2001, 54, 491.
- Pattanayak, D. K. *Mater Sci Eng C* 2009, 29, 1709.
- Mousa, W. F.; Kobayashi, M.; Shinzato, S.; Kamimura, M.; Neo, M.; Yoshihara, S.; Nakamura, T. *Biomaterials* 2000, 21, 2137.
- Kokubo, T. *Biomaterials* 1991, 12, 155.
- Ohura, K.; Nakamura, T.; Yamamuro, T.; Kokubo, T.; Ebisawa, Y.; Kotoura, Y.; Oka, M. *J Biomed Mater Res* 1991, 25, 357.
- Ohtsuki, C.; Kushitani, H.; Kokubo, T.; Kotani, S.; Yamamuro, T. *J Biomed Mater Res* 1991, 25, 1363.
- Cao, W.; Hench, L. L. *Ceram Int* 1996, 22, 493.
- ASTM D 790-03. *Standard Test Methods for Flexural Properties of Unreinforced and Reinforced Plastics and Electrical Insulating Materials*; ASTM International: West Conshohocken, PA, 2005.
- Vallo, C. I. *J Biomed Mater Res* 2000, 53, 717.
- Morejón, L.; Mendizábal, A. E.; García-Menocal, J. A. D.; Ginebra, M. P.; Aparicio, C.; Mur, M. J. G.; Marsal, M.; Davidenko,



- N.; Ballesteros, M. E.; Planell, J. A. *J Biomed Mater Res Part B: Appl Biomater* 2005, 72, 345.
19. Vallo, C. I.; Montemartini, P. E.; Fanovich, M. A.; Porto López, J. M.; Cuadrado, T. R. *J Biomed Mater Res* 1999, 48, 150.
20. Goto, K.; Tamura, J.; Fujibayashi, S.; Hashimoto, M.; Kawashita, M.; Kokubo, T.; Nakamura, T. *Biomaterials* 2005, 26, 6496.
21. Yang, J. M.; Shyu, J.; Chen, H. L. *Polym Eng Sci* 1998, 38, 530.
22. Cheng, S.; Lau, K.; Liu, T.; Zhao, Y.; Lam, P.; Yin, Y. *Compos B* 2009, 40, 650.
23. Hameed, N.; Sreekumar, P. A.; Francis, B.; Yang, W.; Thomas, S. *Compos A: Appl SciManufact* 2007, 38, 2422.
24. Khaled, S. M. Z.; Miron, R. J.; Hamilton, D. W.; Charpentier, P. A.; Rizkalla, A. S. *Dent Mater* 2010, 26, 169.